Identification and Characterization of Persistent Intracellular Human Immunodeficiency Virus Type 1 Integrase Strand Transfer Inhibitor Activity[∇][†]

Yasuhiro Koh, Hillel Haim, and Alan Engelman*

Department of Cancer Immunology and AIDS, Dana-Farber Cancer Institute, and Division of AIDS, Harvard Medical School, Boston, Massachusetts 02115

Pharmacokinetic and pharmacodynamic considerations significantly impact infectious disease treatment options. One aspect of pharmacodynamics is the postantibiotic effect, classically defined as delayed bacterial growth after antibiotic removal. The same principle can apply to antiviral drugs. For example, significant delays in human immunodeficiency virus type 1 (HIV-1) replication can be observed after nucleoside/nucleotide reverse transcriptase inhibitor (N/NtRTI) removal from culture medium, because these prodrugs must be anabolized into active, phosphorylated forms once internalized into cells. A relatively new class of anti-HIV-1 drugs is the integrase strand transfer inhibitors (INSTIs), and the INSTIs raltegravir (RAL) and elvitegravir (EVG) were tested here alongside positive N/NtRTI controls tenofovir disoproxil fumarate (TDF) and azidothymidine (AZT), as well as the nonnucleoside reverse transcriptase inhibitor negative control nevirapine (NVP), to assess potential postantiviral effects. Transformed and primary CD4-positive cells pretreated with INSTIs significantly resisted subsequent challenge by HIV-1, revealing the following hierarchy of persistent intracellular drug strength: TDF > EVG ∼ AZT > RAL > NVP. A modified time-of-addition assay was moreover developed to assess residual drug activity levels. Approximately 0.8% of RAL and 2% of initial EVG and TDF 1-h pulse drug levels persisted during the acute phase of HIV-1 infection. EVG furthermore displayed significant virucidal activity. Although there is no reason to suspect obligate intracellular modification, this study nevertheless defines significant intracellular persistence of prototype INSTIs. Ongoing second-generation formulations should therefore consider the potential for significant postantiviral effects among this drug class. Combined intracellular persistence and virucidal activities suggest potential pre-exposure prophylaxis applications for EVG.

Human immunodeficiency virus type 1 (HIV-1) is the etiological agent of the worldwide AIDS epidemic (24). Virus replication proceeds through a number of well-defined steps, many of which are targeted by antiviral drugs. Infection begins when the gp120 envelope glycoprotein engages the CD4 receptor and a chemokine coreceptor (CCR5 or CXCR4) on the cell surface. Following a series of conformational changes, the viral transmembrane glycoprotein inserts into the plasma membrane to initiate virus-cell fusion. After entry and uncoating, the reverse transcriptase (RT) enzyme along with its associated RNase H activity synthesizes double-stranded linear DNA, using the viral RNA genome as template. Soon thereafter the integrase enzyme processes the 3′ ends of the viral DNA in lieu of chromosomal DNA integration. The resulting preintegration nucleoprotein complex transports the DNA and associated proteins to the nucleus, where integrase catalyzes its second activity, DNA strand transfer. The integrated provirus is the transcriptional template for the synthesis of spliced as well as genome-length mRNAs. Following nuclear export and translation, viral structural proteins and two copies of full-length mRNA coalesce at the cellular membrane to initiate virus assembly. The viral protease digests Gag and Gag-Pol polyprotein precursors during assembly and virus release to yield the mature, infectious virus particle. See reference 23 for several chapters that highlight recent advances in the molecular virology of HIV-1 replication.

Over 25 antiretroviral drugs and drug combinations are approved for treating HIV-1 infection, with the majority falling into one of three classes (45). Nucleoside/nucleotide RT inhibitors (NRTIs/NtRTIs) and nonnucleoside RT inhibitors (NNRTIs) target reverse transcription, whereas protease inhibitors (PIs) thwart the processing of viral protein precursors into constituent virion components. In terms of other drug classes, two inhibitors block different aspects of virus entry: enfuvirtide targets transmembrane envelope glycoprotein function, whereas maraviroc is a CCR5 antagonist. Raltegravir (RAL) is the sole approved integrase inhibitor (43). Because it as well as numerous other drugs in development preferentially inhibit DNA strand transfer activity, the compounds define the integrase strand transfer inhibitor (INSTI) class of anti-HIV-1 drugs (30). Elvitegravir (EVG) is another well-studied INSTI (22, 41).

Pharmacokinetic (PK) and pharmacodynamic (PD) parameters significantly influence the course of antiviral treatment (9, 42), as highlighted for RAL by correlating the minimal daily dose with maximum protection (20, 29). PK/PD analysis moreover revealed that patients harboring plasma RAL concentra-

* Corresponding author. Mailing address: Department of Cancer Immunology and AIDS, Dana-Farber Cancer Institute, 44 Binney Street, CLS-1010, Boston, MA 02115. Phone: (617) 632-4361. Fax: (617) 632-3113. E-mail: alan_engelman@dfci.harvard.edu.

tions at 12 h postdosing that were lower than the effective concentration required to inhibit 95% (the EC_{95}) of HIV-1 replication *ex vivo* nevertheless experienced the same treatment success rates as other individuals (47). One possible explanation for this observation is the so-called postantibiotic (in this case, postantiviral) effect. Coined from the antibiotic literature, this term refers to the regrowth delay observed for bacteria after withdrawal of certain drugs, notably, aminoglycosides (6, 27). The same concept applies to antiviral therapy: cells pretreated with NRTIs/NtRTIs, for example, can significantly resist subsequent HIV-1 challenge because these prodrugs enter into obligate intracellular anabolic pathways for conversion to active phosphorylated forms (3, 35, 39). Plasma drug concentrations dictate NNRTI and PI PK behavior, whereas the intracellular half-life is accordingly the key NRTI/NtRTI PK parameter (39, 45). Here, the INSTIs RAL and EVG were compared alongside NRTI/NtRTI and NNRTI control compounds under a number of assay conditions to assess potential postantiviral effect (PAE). Virucidal activities were also determined to address if binding to virus particles contributes to the PK/PD behavior of RAL in patients (47). Our results reveal significant PAEs for both RAL and EVG, although EVG was consistently more durable. EVG, moreover, displayed significant virucidal activity.

MATERIALS AND METHODS

Cells. HeLa-T4 (28) and 293T cells were grown in Dulbecco's modified Eagle's medium (DMEM) supplemented to contain 10% fetal bovine serum (FBS), 100 IU/ml penicillin, and 100 μg/ml streptomycin. Peripheral blood mononuclear cells (PBMC) purified from the blood of HIV-1-negative donors by Ficoll-Paque density gradient centrifugation were stimulated with 10 μg of phytohemagglutinin (PHA; Sigma-Aldrich, St. Louis, MO) per ml for 2 days and then cultured in RPMI 1640 medium supplemented with 10% FBS, 100 IU/ml penicillin, 100 μg/ml streptomycin, and 10 U/ml interleukin-2 (Sigma-Aldrich). Monocyte-derived macrophages (MDM) purified from 10^6 PBMC by plastic adherence in 48-well plates were cultured for 5 days in RPMI 1640 medium supplemented with 10% pooled human sera (Sigma-Aldrich), 100 IU/ml penicillin, 100 μg/ml streptomycin, and 12.5 ng/ml macrophage colony-stimulating factor (R&D Systems, Inc., Minneapolis, MN) (11, 12).

Antiviral agents. RAL was kindly provided by Merck & Co., Inc. (Whitehouse Station, NJ). EVG obtained from Selleck Chemicals (Houston, TX) was used in the majority of experiments; EVG was also purchased from Toronto Research Chemicals (North York, Ontario) and Santa Cruz Biotechnology, Inc. (Santa Cruz, CA). Azidothymidine (AZT), nevirapine (NVP), efavirenz (EFV), and tenofovir disoproxil fumarate (TDF) were obtained through the NIH AIDS Research and Reference Reagent Program (Germantown, MD). Drug cytotoxicity on HeLa-T4 cells was determined by the WST-1 assay (Roche Applied Science, Indianapolis, IN).

Viruses and infections. Single-round HIV-$1_{NLX.Luc.R-}$, which harbors inactivating mutations in *env* and *vpr* and carries the firefly luciferase gene in place of *nef*, was pseudotyped by cotransfecting 293T cells with expression plasmids encoding either the vesicular stomatitis virus G protein (VSV-G) or HIV-1_{NL4-3} envelope protein as described previously (26). Alternatively, HIV-$1_{NLX.Luc.R+}$ was pseudotyped with the dual-tropic glycoprotein derived from HIV-$1_{89.6}$ (26). The D64N/D116N (N/N) HIV-$1_{NLX.Luc.R-}$ mutant contained two inactivating mutations in the integrase active site (34).

Cell-free virus titers were determined using an exogenous RT assay as described previously (34). HeLa-T4 cells (24,000 plated the prior day in 48-plate wells) infected in duplicate with 10^5 cpm of RT activity (RT-cpm) in 0.2 ml at 37°C were washed at 2 h postinfection to remove unbound virus. At 48 h postinfection, cells were lysed and the resulting luciferase activity level was normalized to the total level of protein in the cell extract as described previously (26). Side-by-side infections conducted with N/N active site mutant virus yielded low-level luciferase activities that were subtracted from those obtained with the wild type to yield integrase-dependent HIV-1 infectivity levels. Unless otherwise noted, drug levels added to cells at the same time as virus were readded to the medium after virus removal.

PHA-activated PBMC (2×10^5) in 0.2-ml volumes inoculated with 10^5 RT-cpm in duplicate for 8 h at 37°C were lysed at 48 h postinfection, whereas MDM infected in duplicate with 10^5 RT-cpm of HIV-$1_{NLX.Luc.R+}$ for 12 h at 37°C were lysed at 72 h postinfection. Luciferase activities derived from integrase active site mutant viral infections of primary cells were nearly identical to those obtained with uninfected cell extracts.

The multiplicity of HIV-$1_{NLX.Luc.R-}$ infection was determined via indirect immunofluorescence. HeLa-T4 cells (48,000) in 24-well glass-bottom plates (MatTek Corporation, Ashland, MA) infected in duplicate with serial dilutions of virus were washed at 2 h postinfection to remove unbound virus. At 48 h postinfection, cells were fixed with 2% paraformaldehyde, permeabilized with 0.1% Triton X-100, and blocked with 5% normal donkey serum. Cells were stained with 20 μg/ml mouse antiluciferase antibody (Sigma-Aldrich) in phosphate-buffered saline containing 5% normal donkey serum for 1 h, followed by a 1:200 dilution of fluorescein isothiocyanate-conjugated rat anti-mouse IgG (eBiosciences, San Diego, CA) for 1 h. Cells mounted with Vectashield containing 4′,6-diamidino-2-phenylindole were visualized at 200× magnification with a fluorescence microscope. Percentages of luciferase-positive cells were analyzed by Image J software.

Magnetite nanoparticles (MNPs) were used in some cases to effect rapid, synchronous infection (14, 40) of HeLa-T4 cells. Virus recovered following dialysis against HS buffer (140 mM NaCl, 10 mM HEPES-NaOH; pH 7.3) for 24 h at 4°C and supplemented with 1.5% FBS was preincubated for 5 min with MNPs (0.5 mg/ml) obtained from Chemicell GmbH (Berlin, Germany) or Boca Scientific, Inc. (Boca Raton, FL). Virus-MNP solutions were added dropwise to cell medium to a final (vol/vol) concentration of 1:13. Following incubation for 2 min in the presence of a magnetic flux density of approximately 1 T, cells washed three or four times to remove unbound material were incubated at 37°C and lysed as described above at 48 h postinfection.

Drug concentrations that suppressed luciferase activity to the EC_{50} and EC_{95} levels were determined using the GROWTH equation in Microsoft Excel 2000 (Mountain View, CA).

Virucidal activity assays. Virus-drug mixtures following 1 h of preincubation at 37°C were incubated with MNPs as above prior to infection or, alternatively, drugs were removed prior to infection by washing the mixtures four times by using a Dynal MPC-S magnetic particle concentrator (Invitrogen, Carlsbad, CA). Washed MNP beads resuspended in serum-free DMEM were added to cells, and infection by use of magnetic field proceeded as above.

RESULTS

Ex vivo **infection system and basal drug activities.** The anti-HIV-1 activities of various inhibitors were initially determined in a simplified infection assay. HIV-$1_{NLX.Luc.R-}$ (HIV-Luc) was utilized for ease of assay readout, as this single-round reporter virus carries the luciferase gene in place of *nef* (26). The challenge cells were HeLa-T4, which harbor the CD4 receptor on their surface (28), although HIV-Luc was notably pseudotyped with the pan-tropic VSV-G envelope glycoprotein for initial experiments. Cells that were infected in duplicate for 2 h with 10^5 RT-cpm of virus (approximate multiplicity of infection, 0.01) in the absence or presence of serial diluted drug concentrations were washed and then replenished with medium containing the same drug concentration. Cell extracts were prepared at 2 days postinfection, and resulting luciferase activities were normalized to total protein concentrations to enable comparisons between duplicate samples as well as independent experiments. Cells were additionally infected with matched RT-cpm levels of integrase active site mutant N/N-Luc virus, which typically yields 0.05 to 0.25% of HIV-Luc infectivity (15, 25) due to the low level of Nef that can be expressed in the absence of functional integration (21). Basal NN-Luc activities in the presence and absence of drugs were subtracted from HIV-Luc values to determine integrase-dependent levels of virus infection.

As expected (19, 43), HIV-Luc was potently inhibited when RAL or EVG was included throughout the 2-day infection

TABLE 1. Antiviral activities of various HIV-1 inhibitors[a]

Drug	Class	EC$_{50}$ (μM)	EC$_{95}$ (μM)	CC$_{50}$ (μM)	SI[b]
RAL	INSTI	0.0084 ± 0.0022	0.090 ± 0.004	>100	>11,904
EVG	INSTI	0.0029 ± 0.0007	0.037 ± 0.004	34.0	11,724
AZT	NRTI	0.077 ± 0.028	0.81 ± 0.09	>100	>1,298
TDF	NtRTI	0.030 ± 0.003	0.50 ± 0.033	>100	>3,333
NVP	NNRTI	0.073 ± 0.044	0.68 ± 0.14	>100	>1,369
EFV	NNRTI	0.0011 ± 0.0005	0.008 ± 0.0004	35.0	31,818

[a] Means ± standard deviations obtained from at least three independent experiments, with each experiment conducted in duplicate.
[b] SI, selectivity index (CC$_{50}$/EC$_{50}$).

time course: EC$_{50}$ values for RAL and EVG were 0.0084 ± 0.0022 μM and 0.0029 ± 0.0007 μM, respectively, whereas respective EC$_{95}$s were 0.090 ± 0.004 μM and 0.037 ± 0.004 μM (means ± standard deviations) (Table 1). The RAL 50% cytotoxicity value (CC$_{50}$), >100 μM, was outside the tested range, yielding a selectivity index (CC$_{50}$/EC$_{50}$) of >11,900. With a CC$_{50}$ of 34 μM, the EVG selectivity index was approximately 11,720. Other drugs used in this study included the NRTI AZT (32), NtRTI TDF (2), and NNRTIs NVP (31) and EFV (48). As expected, each drug potently inhibited HIV-Luc, yielding the following EC$_{50}$ and EC$_{95}$ values: AZT, 0.077 ± 0.028 and 0.81 ± 0.09 μM; TDF, 0.030 ± 0.003 and 0.50 ± 0.033 μM; NVP, 0.073 ± 0.044 and 0.68 ± 0.14 μM; EFV, 0.0011 ± 0.0005 and 0.008 ± 0.0004 μM (Table 1). The CC$_{50}$s of AZT, TDF, and NVP were similar to RAL in that they each exceeded 100 μM, whereas EFV, like EVG, had a CC$_{50}$ of approximately 35 μM (Table 1).

RAL and EVG exert their effects at a time coincident with HIV-1 integration. A time-of-addition (TOA) assay was utilized to further characterize INSTI behavior under these conditions. The amount of time at which each drug was added to an ongoing infection was varied (8, 37) in order to define the interval needed for 50% escape from inhibition. RAL and EVG were analyzed at the equal effective concentration of 10× the EC$_{95}$ (Table 1) alongside control compounds to determine their TOA profiles. The addition of AZT could be

delayed for about 4.8 h before 50% loss in potency was observed, whereas NVP required about 7.2 h to reveal this effect (Fig. 1A). These data, which agree well with previous observations (8), reflect the need for AZT conversion to its active phosphorylated form (3), which NVP does not require. RAL addition could be postponed for about 10.2 h before 50% loss in activity was observed, whereas EVG required about 11.1 h (Fig. 1A). Titrating RAL and EVG over a 10-fold range (from 10× to 100× the EC$_{95}$) did not significantly affect the resulting time windows (10.1 to 12.7 h for 50% inhibition) (Fig. 1B). MNP-mediated infection in the presence of 10 μM RAL (11.1× the EC$_{95}$) (Table 1) moreover revealed 11.1 h as the 50% inhibition time point (data not shown). We therefore conclude that RAL and EVG exert their antiviral affects from approximately 10 to 13 h postinfection. These results agree well with analyses of other preclinical integrase inhibitors (7, 36) and help fine-tune the RAL functional window, previously reported as >7 h from the start of infection (18).

Intracellular persistence of antiviral compounds. To address the intracellular persistence of the various inhibitors, cells pretreated with 100× the EC$_{95}$ of each drug for 24 h were washed three times to remove unincorporated compounds from the culture medium prior to infection. Virus was added immediately after washing or 2, 4, 8, or 12 h thereafter. Following the standard format, cells thrice washed after 2 h to remove unbound virus were lysed at 48 h from the start of infection. Control compounds included NVP, which does not persist in cells (1), and AZT and TDF, which display persistence due to prodrug conversion to active phosphorylated forms once internalized (3, 39). Accordingly, cells infected immediately after AZT removal supported about 18% of the level of infection of non-drug-treated cells (Fig. 2). Thus, even though AZT inhibits reverse transcription at about 5 h postinfection (Fig. 1A), effective intracellular levels persisted after the drug was removed from the medium prior to infection. Delaying the infection for 2 to 4 h after drug removal yielded about 40% of the control level of infection, whereas a further 8 h of delay failed to yield residual AZT activity (Fig. 2). TDF, by contrast, was impressively effective at inhibiting HIV-Luc
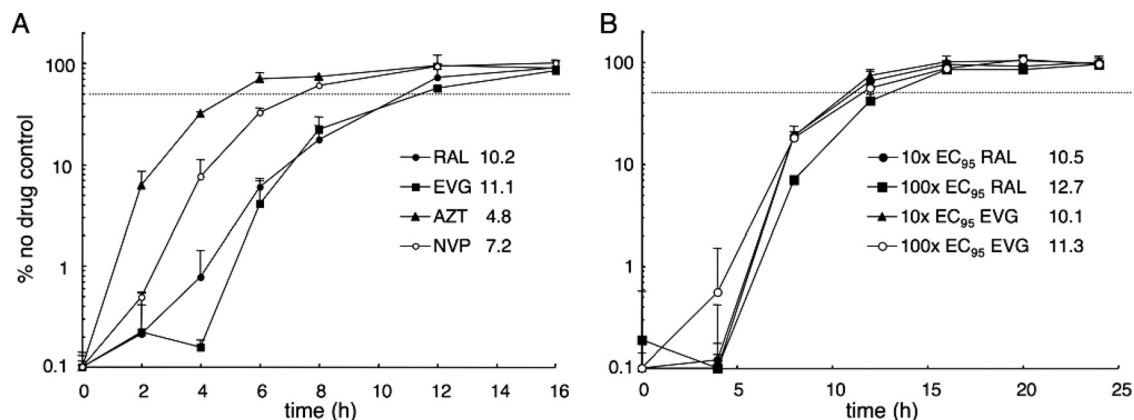

FIG. 1. Functional windows of antiviral drug action. (A) At the indicated times, 10-fold EC$_{95}$ adjusted levels of RAL, EVG, AZT, or NVP were added to HIV-Luc-infected cultures. Cells were lysed at 48 h postinfection, and luciferase activities are expressed as the percentage of the response in non-drug-treated cells. (B) Results of an experiment similar to that in panel A, except cells were treated with 10× the EC$_{95}$ of RAL, 100× the EC$_{95}$ of RAL, 10× the EC$_{95}$ of EVG, or 100× the EC$_{95}$ of EVG at the indicated times. Numbers indicate the time (in h) required for 50% inhibition compared to the no-drug control (dashed lines).
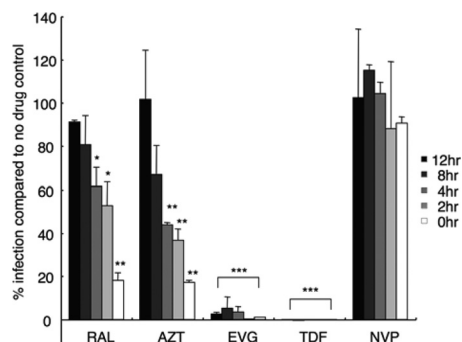
FIG. 2. Functional intracellular persistence of HIV-1 inhibitors. Cells exposed to $100\times$ the EC_{95} levels of each compound for 24 h were washed to deplete extracellular drug, cultured for various time periods (0, 2, 4, 8, or 12 h), exposed to HIV-Luc, and then further cultured for 48 h prior to cell lysis. $*$, $P < 0.05$; $**$, $P < 0.01$; $***$, $P < 0.001$ compared to the no-drug control (based on Student's t test).

activity even when the cells were infected 12 h after compound washout. On the flip side, NVP failed to effectively inhibit HIV-Luc, even when the cells were infected immediately after drug removal (Fig. 2). These results define TDF and NVP as strict positive and negative drug washout controls, with AZT scoring betwixt these extremes.

RAL behaved similarly to AZT under these conditions: infecting cells immediately after RAL washout yielded about 19% of the level of the non-drug-treated control, whereas additional 2- to 4-h delays prior to infection yielded about 50 to 60% of the control value (Fig. 2). Statistical significance, though, was lost when the time from RAL washout to infection was delayed by 8 to 12 h. EVG interestingly behaved as a relatively persistent chemical under these conditions, mimicking the TDF positive control, more so than did either RAL or AZT (Fig. 2). We therefore conclude that each INSTI functionally persists intracellularly, with EVG lingering more so than RAL (Fig. 2). A new EC_{50}, which we refer to as the washout EC_{50}, was calculated based on data acquired when cells were infected immediately after drug removal (Table 2). Washout EC_{50}s ranged from a low of 0.06 ± 0.04 μM for EVG to a high of >100 μM for NVP. Normalizing washout EC_{50}s to the values obtained under standard drug treatment conditions (Table 1) revealed that TDF was the most persistent compound, followed by EVG and AZT (Table 2, EC_{50} adjusted ratios). Although its EC_{50} adjusted value was about 9-fold higher than AZT, RAL nonetheless behaved in a distinguishable manner from the NVP negative control under these conditions (Fig. 2 and Table 2).

Due to the relative strength of intracellular EVG persistence, compounds obtained from two additional sources were analyzed alongside the Selleck Company reagent. Because all three commercial lots behaved similarly (see Table S1 in the supplemental material), we conclude that functional intracellular retention under these culture conditions is an inherent chemical property of EVG.

Virucidal activities of INSTIs. MNPs were employed to determine inhibitory potentials of virus-bound drugs, also known as virucidal activity. This experimental format afforded extensive washing of HeLa-T4 cell monolayers to remove unbound virus and drug after just 2 min of infection (14). Before moving

to inhibitor studies, the efficiency of MNP-mediated infection was analyzed. As shown in Fig. 3A, 2 min of MNP-mediated infection was actually more efficient than the standard 2-h diffusion format. Washing after just 2 min of diffusion in the absence of MNPs yielded negligible infectivity.

HIV-Luc was preincubated for 1 h at 37°C with various concentrations of RAL and EVG versus NVP and EFV control compounds. NVP acts in rapid equilibrium under conditions whereby EFV binds tightly to virions through an interaction with its RT target (33). As expected, EFV inhibited HIV-Luc infectivity in a dose-dependent manner (Fig. 3B). The apparent EC_{50} under these conditions, ~ 1 μM, agreed well with previous diffusion-based measurements (33), validating the use of MNPs in this format. RAL function mirrored that of NVP under these conditions; although statistically relevant effects were observed at relatively high drug concentrations, these clearly differed from EFV. EVG, by contrast, yielded a clear dose-dependent response, similar to the results observed with EFV (Fig. 3B). The apparent EC_{50} of 3.4 μM reveals a previously unrecognized virucidal activity for this INSTI. In an alternative format of the assay, MNP-conjugated virus-drug mixtures were washed extensively to remove unbound drug prior to infection (46). Under these conditions, EFV and EVG inhibited HIV-Luc infectivity, with EC_{50}s of approximately 0.8 and 12 μM, respectively, whereas neither RAL nor NVP displayed significant activity (see Fig. S1 in the supplemental material). We conclude that RAL and EVG possess significantly different virucidal activities (Fig. 3B; see also Fig. S1).

Inhibitor action window and intracellular persistence revealed in a modified TOA assay. The TOA method was modified to a pulse format by taking advantage of synchronous MNP-mediated entry. At various times after the initial 2 min of infection, cells were pulsed with $100\times$ the EC_{95} of test compound for 1 h. After three washes, cells were incubated in the absence of drug for the remainder of the infection time course. NVP was most effective when added at 3 h postinfection, yielding about 23% of the level of infectivity observed with the no-drug control at the resulting 4-h time point (Fig. 4). This result was consistent with the relatively rapid turnover of NVP in cells: the optimal pulse coincided with the presence of the targeted replication intermediate, the reverse transcription complex at 3 to 4 h postinfection, and was moreover only partially effective at inhibiting virus infectivity. Due to its effective intracellular persistence (Fig. 2 and Table 2), the initial 1-h TDF pulse, in stark contrast to NVP, permitted only about 0.36% residual infectivity, an effect that gradually diminished with later TDF pulses (Fig. 4). Based on these data sets, we

TABLE 2. Antiviral activities following drug washout[a]

Drug	Washout EC_{50} (μM)	EC_{50} adjusted ratio[b]
RAL	4.6 ± 1.8	547.6
EVG	0.06 ± 0.04	20.7
AZT	4.6 ± 2.9	59.7
TDF	0.12 ± 0.06	4.0
NVP	>100	$>1,370$

[a] Means $\pm$ standard deviations of a minimum of three independent experiments, with each conducted in duplicate.
[b] Washout EC_{50}/standard EC_{50} ratio (see Table 1).
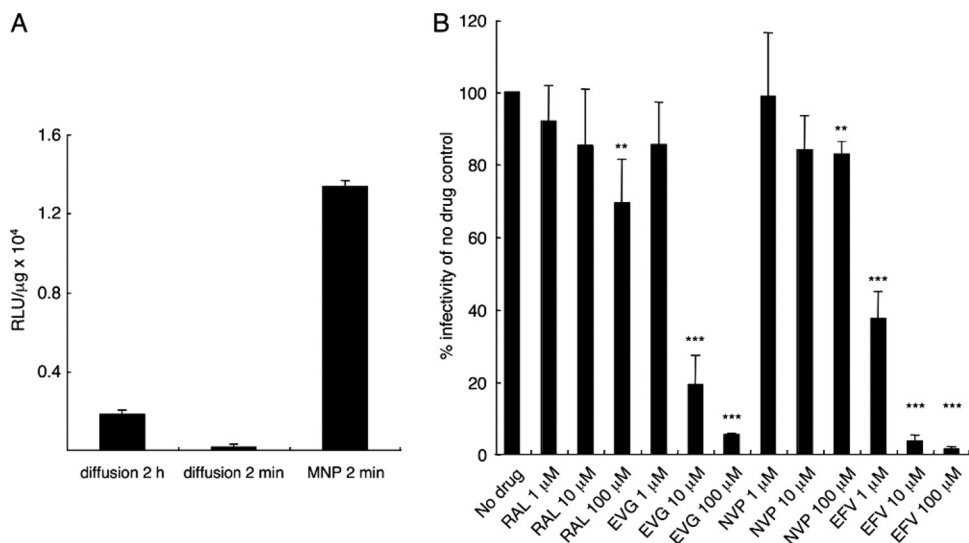
FIG. 3. Virucidal activities of anti-HIV-1 compounds. (A) Normalized HIV-Luc infectivities following standard 2-h absorption, shortened 2-min absorption, or 2 min of MNP-mediated infection. (B) HIV-Luc was preincubated with the indicated level of drug for 1 h prior to 2 min of MNP-mediated infection. Extensively washed cultures were incubated in the absence of drug for 2 days prior to cell lysis and luciferase assays. The NN-luc control virus was omitted from the virucidal activity assays. ∗∗, $P < 0.01$; ∗∗∗, $P < 0.001$ compared to the no-drug control (based on Student's t test). RLU, relative light units.

conclude that reverse transcription was effectively completed by 11 h postinfection under these conditions.

The INSTIs behaved like TDF in that their earliest pulses yielded the greatest antiviral effects (Fig. 4). Because the initial RAL pulse permitted about 9% residual infectivity, we conclude that about 73 nM RAL (the EC_{91} [Table 1]), or about 0.8% of the pulsed drug level, functionally persisted. Consistent with the results obtained via the traditional TOA format (Fig. 1), the 11-h RAL and EVG pulses suppressed infection about 2-fold compared to the no-drug control. Consistent with the relatively persistent behavior of EVG in previous experi-
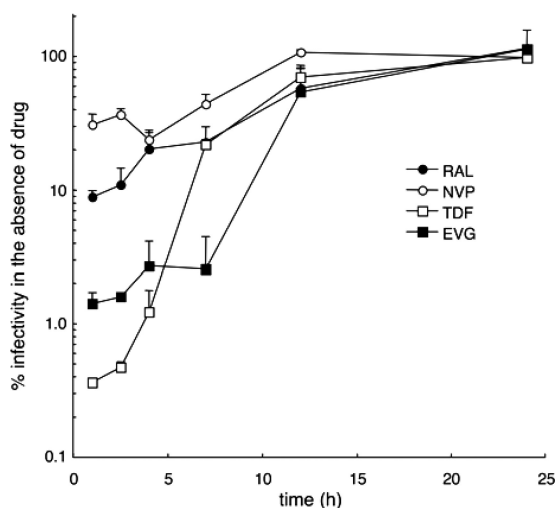
ments (Fig. 2 and Table 2), HIV-Luc accomplished only about 1.4% of the level of the no-drug condition after the initial 1-h drug pulse (Fig. 4). Considering a corresponding $EC_{98.6}$ value of 75 nM (Table 1), about 2% of the initial EVG pulse persisted under these conditions. Although the initial 1-h TDF pulse yielded a somewhat greater antiviral affect (Fig. 4), the corresponding $EC_{99.6}$ value of 0.95 μM likewise revealed about 1.9% of the initial TDF pulse functionally persisted.

Antiviral activities in primary cells. The HeLa-T4 cell line afforded a relatively easy-to-manipulate system for initial investigations into INSTI behavior *ex vivo*. Because HIV-1 primarily infects $CD4^+$ T cells and macrophages *in vivo* (5), we felt it necessary to also characterize INSTI persistence in primary $CD4^+$ target cells. PBMC obtained from human blood donors were either stimulated with PHA/interleukin-2 or differentiated into MDM as described previously (11, 12, 34). HIV-Luc was engineered to harbor the $HIV-1_{NL4-3}$ envelope glycoprotein for effective PBMC infection, whereas the Vpr-expressing variant of HIV-Luc was pseudotyped with the dual-tropic 89.6 envelope for macrophage cell infection (26). The PBMC infection time course, as for HeLa-T4 cells, covered 2 days, whereas MDM infections lasted for 3 days. Experiments conducted in the presence of drug throughout the time courses revealed potent INSTI activities in primary cells. Comparing the data presented in Table 3 to results shown in Table 1, RAL was 2- to 3-fold more potent based on EC_{50}s, whereas EVG was 6- to 10-fold more active. NVP was likewise 2- to 3-fold more potent, whereas TDF was equally or somewhat less potent in primary cells compared to HeLa-T4 cells.

To assess intracellular drug persistence, PBMC or MDM cells pretreated with compounds for 24 h were extensively washed and then infected in the absence of drug. Two to 3 days later, cells were lysed and infectivities were assessed as normalized luciferase values. The results of these experiments

FIG. 4. TOA pulse assay. RAL, EVG, TDF, or NVP (100× the EC_{95} adjusted) was removed from infected cultures at the indicated time points after a 1-h pulse. Thereafter, rewashed cells were incubated prior to lysis at 48 h postinfection. Results shown are the percent infectivity in comparison to no-drug controls.

TABLE 3. Antiviral activities in primary human cells

Drug	Mean ± SD EC value (μM)[a] in:			
	PBMC		MDM	
	EC_{50}	EC_{95}	EC_{50}	EC_{95}
RAL	0.0024 ± 0.0004	0.048 ± 0.009	0.0043 ± 0.0017	0.080 ± 0.020
EVG	0.0003 ± 0.0001	0.0074 ± 0.0013	0.0005 ± 0.0003	0.0082 ± 0.0008
TDF	0.046 ± 0.018	0.72 ± 0.07	0.028 ± 0.013	0.52 ± 0.32
NVP	0.041 ± 0.019	0.69 ± 0.03	0.027 ± 0.016	0.64 ± 0.11

[a] Means and standard deviations obtained from three independent experiments, with each experiment conducted in duplicate.

TABLE 4. Drug persistence in primary cell types[a]

Drug	PBMC		MDM	
	Washout EC_{50} (μM)	EC_{50} adjusted ratio[b]	Washout EC_{50} (μM)	EC_{50} adjusted ratio[b]
RAL	3.3 ± 0.6	1,375	4.9 ± 0.7	1,140
EVG	0.036 ± 0.016	120	0.025 ± 0.015	50
TDF	0.055 ± 0.039	1.2	0.034 ± 0.019	1.2
NVP	>100	>2,439	>100	>3,703

[a] Averages ± standard deviations of three independent experiments, with infections within each experiment conducted in duplicate.
[b] Washout EC_{50}/standard EC_{50} ratio (see Table 3).

revealed numbers that were in large part similar to the data reaped from HeLa-T4 cells (compare Table 4 to Table 2). TDF was remarkably potent under these conditions, yielding washout EC_{50}s that were only 1.2-fold different from the values obtained when the drug was present throughout the infections (compare Table 4 to Table 3). As expected, NVP failed to score in either primary cell drug washout assay (Table 4).

RAL washout EC_{50}s in PBMC and MDM, 3.3 μM and 4.9 μM, respectively, were basically the same as the 4.6 μM value obtained in HeLa-T4 cells. The primary cell adjusted EC_{50}s were accordingly about 2-fold less potent than the HeLa-T4 cell value. Based on drug concentration, about half as much EVG defined washout EC_{50}s in primary compared to HeLa-T4 cells. Due to the relative strength of this INSTI in primary cells, the EC_{50} adjusted values were, however, about 2.5- to 6-fold less potent than the corresponding HeLa-T4 cell value (Tables 2 and 4). We conclude that EVG persists relatively well in primary cells, whereas RAL, although significantly less potent than EVG, nevertheless appears to be a persistent compound after drug washout (Table 4).

DISCUSSION

Our results reveal a hitherto-unknown property of two prototype INSTIs, their ability to protect cells from HIV-1 infection *ex vivo* after drug removal from the culture medium (Fig. 2 and 4; Tables 2 and 4). EVG, moreover, consistently outshined RAL under these assay conditions. After adjusting for inherent drug strength, EVG persisted in HeLa-T4 cells about 19% as efficiently as the TDF positive control (Table 2). This PAE, though, fell to about 1 to 2% of relative TDF strength in primary PBMC and MDM (Table 4). RAL displayed only about 0.1 to 0.7% of the relative TDF PAE in HeLa-T4 and primary cells (Tables 2 and 4).

Considering that the 50% inhibitory concentration of EVG under certain *in vitro* DNA strand transfer assay conditions is 1.7 nM (4), there is little reason to suspect that the antiviral function requires intracellular drug modification (Table 1). What might then contribute to the PAE associated with this compound? We speculate that EVG is lost from dividing and nondividing target cells at a relatively low rate due to binding to a component in common among HeLa-T4 cells, PBMC, and MDM. Drug function moreover must persist after this hypothetical binding transpires. To test if limited chemical solubility contributed to EVG extracellular precipitation and binding to cell surface proteins in a manner that precluded subsequent removal through washing, PBMC preexposed to EVG or TDF were either washed as before or washed, trypsinized, and then

rewashed prior to infection. Because indistinguishable levels of HIV-Luc infectivity were observed under both conditions (see Fig. S2 in the supplemental material), we conclude that EVG needs to be internalized to mediate its PAE. Additional work could potentially identify the cellular component(s) that apparently binds EVG and prolongs its intracellular antiviral activity. Chemical modifications that reduce binding might reduce the cytotoxicity of future compounds. Alternatively, changes that increase binding could increase potency if the PAE could be improved without significantly increasing drug toxicity. The PAE and virucidal activities described herein might possibly contribute to the relative efficacy of EVG in clinical trials (22). We moreover note that the naphthyridine carboxamide INSTI L-870812 (16) has shown some promise as a topical microbicide component (C. Dobard and W. Heneine, presented at the 2010 International Conference on Microbicides, Pittsburgh, PA, 22 to 25 May 2010). Given the potential added benefits of PAE and virucidal activities to microbicidal efficacy, it may be worth testing EVG in this context.

The relatively weak PAE associated with RAL is unlikely to contribute significantly to the successful treatment course observed for the patients that harbored $<EC_{95}$ plasma drug concentrations at 12 h postdosing (47). Moreover, we failed to detect any appreciable functional interaction between RAL and HIV-1 (Fig. 3; see also Fig. S1 in the supplemental material), ruling out that tight binding to integrase in virions contributes significantly to the favorable PK/PD outlook in patients. The RAL washout EC_{50} was additionally measured in resting PBMC to determine if the relative quiescent state of these cells and/or associated low rates of reverse transcription and integration (38, 44) might increase the apparent PAE. Because this experiment yielded a value of 7.2 μM (data not shown), we conclude that neither cellular activation nor division status contributes significantly to functional intracellular RAL persistence.

Predecessor INSTIs preferentially interacted with the integrase-viral DNA complex compared to free integrase protein *in vitro* (10). It therefore seems reasonable to assume that these drugs interact tightly with the preintegration complex that forms during virus infection. Recent analyses of interactions between INSTIs and wild-type and drug-resistant integrase-viral DNA complexes *in vitro* indeed have indicated that the drug dissociation rate is a key predictor of *in vivo* pharmacological utility (13, 17). It therefore seems possible that the half-life of RAL dissociation from the integrase-DNA complex may be the decisive PK parameter of this drug. Additional work is required to determine if this will apply equally across

the INSTIs, or whether the PAE and virucidal activities described herein might be important factors for certain members of this relatively new drug class.

REFERENCES

1. **Azoulay, S., M.-C. Nevers, C. Creminon, L. Heripret, J. Durant, P. Dellamonica, J. Grassi, R. Guedj, and D. Duval.** 2004. Sensitive enzyme immunoassay for measuring plasma and intracellular nevirapine levels in human immunodeficiency virus-infected patients. Antimicrob. Agents Chemother. **48:**104–109.
2. **Balzarini, J., A. Holy, J. Jindrich, L. Naesens, R. Snoeck, D. Schols, and E. De Clercq.** 1993. Differential antiherpesvirus and antiretrovirus effects of the (S) and (R) enantiomers of acyclic nucleoside phosphonates: potent and selective in vitro and in vivo antiretrovirus activities of (R)-9-(2-phosphonomethoxypropyl)-2,6-diaminopurine. Antimicrob. Agents Chemother. **37:**332–338.
3. **Balzarini, J., L. Naesens, S. Aquaro, T. Knispel, C. Perno, E. De Clercq, and C. Meier.** 1999. Intracellular metabolism of CycloSaligenyl 3′-azido-2′,3′-dideoxythymidine monophosphate, a prodrug of 3′-azido-2′,3′-dideoxythymidine (zidovudine). Mol. Pharmacol. **56:**1354–1361.
4. **Bar-Magen, T., R. D. Sloan, V. H. Faltenbacher, D. A. Donahue, B. D. Kuhl, M. Oliveira, H. Xu, and M. A. Wainberg.** 2009. Comparative biochemical analysis of HIV-1 subtype B and C integrase enzymes. Retrovirology **6:**103.
5. **Collman, R.** 1992. Human immunodeficiency virus type 1 tropism for human macrophages. Pathobiology **60:**213–218.
6. **Craig, W. A.** 1993. Post-antibiotic effects in experimental infection models: relationship to in-vitro phenomena and to treatment of infections in man. J. Antimicrob. Chemother. **31**(Suppl. D):149–158.
7. **Daelemans, D., R. Lu, E. De Clercq, and A. Engelman.** 2007. Characterization of a replication-competent, integrase-defective human immunodeficiency virus (HIV)/simian virus 40 chimera as a powerful tool for the discovery and validation of HIV integrase inhibitors. J. Virol. **81:**4381–4385.
8. **De Clercq, E., N. Yamamoto, R. Pauwels, M. Baba, D. Schols, H. Nakashima, J. Balzarini, Z. Debyser, B. A. Murrer, D. Schwartz, D. Thornton, G. Bridger, S. Fricker, G. Henson, M. Abrams, and D. Picker.** 1992. Potent and selective inhibition of human immunodeficiency virus (HIV)-1 and HIV-2 replication by a class of bicyclams interacting with a viral uncoating event. Proc. Natl. Acad. Sci. U. S. A. **89:**5286–5290.
9. **Drusano, G. L.** 1993. Pharmacodynamics of antiretroviral chemotherapy. Infect. Control Hosp. Epidemiol. **14:**530–536.
10. **Espeseth, A. S., P. Felock, A. Wolfe, M. Witmer, J. Grobler, N. Anthony, M. Egbertson, J. Y. Melamed, S. Young, T. Hamill, J. L. Cole, and D. J. Hazuda.** 2000. HIV-1 integrase inhibitors that compete with the target DNA substrate define a unique strand transfer conformation for integrase. Proc. Natl. Acad. Sci. U. S. A. **97:**11244–11249.
11. **Gorry, P. R., G. Bristol, J. A. Zack, K. Ritola, R. Swanstrom, C. J. Birch, J. E. Bell, N. Bannert, K. Crawford, H. Wang, D. Schols, E. De Clercq, K. Kunstman, S. M. Wolinsky, and D. Gabuzda.** 2001. Macrophage tropism of human immunodeficiency virus type 1 isolates from brain and lymphoid tissues predicts neurotropism independent of coreceptor specificity. J. Virol. **75:**10073–10089.
12. **Gray, L., M. Roche, M. J. Churchill, J. Sterjovski, A. Ellett, P. Poumbourios, S. Sherieff, B. Wang, N. Saksena, D. F. Purcell, S. Wesselingh, A. L. Cunningham, B. J. Brew, D. Gabuzda, and P. R. Gorry.** 2009. Tissue-specific sequence alterations in the human immunodeficiency virus type 1 envelope favoring CCR5 usage contribute to persistence of dual-tropic virus in the brain. J. Virol. **83:**5430–5441.
13. **Grobler, J. A., P. M. Mckenna, S. Ly, K. A. Stillmock, C. M. Bahnck, R. M. Danovich, G. Dornadula, D. J. Hazuda, and M. D. Miller.** 2009. HIV integrase inhibitor dissociation rates correlate with efficacy in vitro. Antivir. Ther. **14**(Suppl. 1):A27.
14. **Haim, H., I. Steiner, and A. Panet.** 2005. Synchronized infection of cell cultures by magnetically controlled virus. J. Virol. **79:**622–625.
15. **Hare, S., F. Di Nunzio, A. Labeja, J. Wang, A. Engelman, and P.**
16. **Cherepanov.** 2009. Structural basis for functional tetramerization of lentiviral integrase. PLoS Pathog. **5:**e1000515.
16. **Hazuda, D. J., S. D. Young, J. P. Guare, N. J. Anthony, R. P. Gomez, J. S. Wai, J. P. Vacca, L. Handt, S. L. Motzel, H. J. Klein, G. Dornadula, R. M. Danovich, M. V. Witmer, K. A. Wilson, L. Tussey, W. A. Schleif, L. S. Gabryelski, L. Jin, M. D. Miller, D. R. Casimiro, E. A. Emini, and J. W. Shiver.** 2004. Integrase inhibitors and cellular immunity suppress retroviral replication in rhesus macaques. Science **305:**528–532.
17. **Hightower, K., R. Wang, and M. Underwood.** 2010. S/GSK1349572 demonstrates significantly slower dissociation rates than raltegravir when comparing wild type and raltegravir resistant integrase protein. International HIV & Hepatitis Virus Drug Resistance Workshop, Dubrovnik, Croatia. Antivir. Ther. **15**(Suppl. 2):A16.
18. **Hombrouck, A., B. Van Remoortel, M. Michiels, W. Noppe, F. Christ, A. Eneroth, B. L. Sahlberg, K. Benkestock, L. Vrang, N. G. Johansson, M. L. Barreca, L. De Luca, S. Ferro, A. Chimirri, Z. Debyser, and M. Witvrouw.** 2008. Preclinical evaluation of 1H-benzylindole derivatives as novel human immunodeficiency virus integrase strand transfer inhibitors. Antimicrob. Agents Chemother. **52:**2861–2869.
19. **Hombrouck, A., A. Voet, B. Van Remoortel, C. Desadeleer, M. De Maeyer, Z. Debyser, and M. Witvrouw.** 2008. Mutations in human immunodeficiency virus type 1 integrase confer resistance to the naphthyridine L-870,810 and cross-resistance to the clinical trial drug GS-9137. Antimicrob. Agents Chemother. **52:**2069–2078.
20. **Iwamoto, M., L. A. Wenning, A. S. Petry, M. Laethem, M. De Smet, J. T. Kost, S. A. Merschman, K. M. Strohmaier, S. Ramael, K. C. Lasseter, J. A. Stone, K. M. Gottesdiener, and J. A. Wagner.** 2008. Safety, tolerability, and pharmacokinetics of raltegravir after single and multiple doses in healthy subjects. Clin. Pharmacol. Ther. **83:**293–299.
21. **Kelly, J., M. H. Beddall, D. Yu, S. R. Iyer, J. W. Marsh, and Y. Wu.** 2008. Human macrophages support persistent transcription from unintegrated HIV-1 DNA. Virology **372:**300–312.
22. **Klibanov, O. M.** 2009. Elvitegravir, an oral HIV integrase inhibitor, for the potential treatment of HIV infection. Curr. Opin. Invest. Drugs **10:**190–200.
23. **Kurth, R., and N. Bannert.** 2010. Retroviruses: molecular biology, genomics and pathogenesis. Caister Academic Press, Norfolk, United Kingdom.
24. **Levy, J. A.** 2009. HIV pathogenesis: 25 years of progress and persistent challenges. AIDS **23:**147–160.
25. **Lu, R., H. Z. Ghory, and A. Engelman.** 2005. Genetic analyses of conserved residues in the carboxyl terminal domain of human immunodeficiency virus type 1 integrase. J. Virol. **79:**10356–10368.
26. **Lu, R., A. Limon, E. Devroe, P. A. Silver, P. Cherepanov, and A. Engelman.** 2004. Class II integrase mutants with changes in putative nuclear localization signals are primarily blocked at a postnuclear entry step of human immunodeficiency virus type 1 replication. J. Virol. **78:**12735–12746.
27. **MacKenzie, F. M., and I. M. Gould.** 1993. The post-antibiotic effect. J. Antimicrob. Chemother. **32:**519–537.
28. **Maddon, P. J., A. G. Dalgleish, J. S. McDougal, P. R. Clapham, R. A. Weiss, and R. Axel.** 1986. The T4 gene encodes the AIDS virus receptor and is expressed in the immune system and the brain. Cell **47:**333–348.
29. **Markowitz, M., J. O. Morales-Ramirez, B. Y. Nguyen, C. M. Kovacs, R. T. Steigbigel, D. A. Cooper, R. Liporace, R. Schwartz, R. Isaacs, L. R. Gilde, L. Wenning, J. Zhao, and H. Teppler.** 2006. Antiretroviral activity, pharmacokinetics, and tolerability of MK-0518, a novel inhibitor of HIV-1 integrase, dosed as monotherapy for 10 days in treatment-naive HIV-1-infected individuals. J. Acquir. Immune Defic. Syndr. **43:**509–515.
30. **McColl, D. J., and X. Chen.** 2010. Strand transfer inhibitors of HIV-1 integrase: bringing IN a new era of antiretroviral therapy. Antiviral Res. **85:**101–118.
31. **Merluzzi, V. J., K. D. Hargrave, M. Labadia, K. Grozinger, M. Skoog, J. C. Wu, C. K. Shih, K. Eckner, S. Hattox, J. Adams, A. S. Rosenthal, R. Faanes, R. J. Eckner, R. A. Koup, and J. L. Sullivan.** 1990. Inhibition of HIV-1 replication by a nonnucleoside reverse transcriptase inhibitor. Science **250:**1411–1413.
32. **Mitsuya, H., K. J. Weinhold, P. A. Furman, M. H. St. Clair, S. N. Lehrman, R. C. Gallo, D. Bolognesi, D. W. Barry, and S. Broder.** 1985. 3′-Azido-3′-deoxythymidine (BW A509U): an antiviral agent that inhibits the infectivity and cytopathic effect of human T-lymphotropic virus type III/lymphadenopathy-associated virus in vitro. Proc. Natl. Acad. Sci. U. S. A. **82:**7096–7100.
33. **Motakis, D., and M. A. Parniak.** 2002. A tight-binding mode of inhibition is essential for anti-human immunodeficiency virus type 1 virucidal activity of nonnucleoside reverse transcriptase inhibitors. Antimicrob. Agents Chemother. **46:**1851–1856.
34. **Nakajima, N., R. Lu, and A. Engelman.** 2001. Human immunodeficiency virus type 1 replication in the absence of integrase-mediated DNA recombination: definition of permissive and nonpermissive T-cell lines. J. Virol. **75:**7944–7955.
35. **Nakata, H., M. Amano, Y. Koh, E. Kodama, G. Yang, C. M. Bailey, S. Kohgo, H. Hayakawa, M. Matsuoka, K. S. Anderson, Y. C. Cheng, and H. Mitsuya.** 2007. Activity against human immunodeficiency virus type 1, intracellular metabolism, and effects on human DNA polymerases of 4′-ethynyl-2-fluoro-2′-deoxyadenosine. Antimicrob. Agents Chemother. **51:**2701–2708.

36. **Pannecouque, C., W. Pluymers, B. Van Maele, V. Tetz, P. Cherepanov, E. De Clercq, M. Witvrouw, and Z. Debyser.** 2002. New class of HIV integrase inhibitors that block viral replication in cell culture. Curr. Biol. **12:**1169–1177.

37. **Pauwels, R., K. Andries, J. Desmyter, D. Schols, M. J. Kukla, H. J. Breslin, A. Raeymaeckers, J. Van Gelder, R. Woestenborghs, J. Heykants, K. Schellekens, M. A. C. Janssen, E. De Clercq, and P. A. J. Janssen.** 1990. Potent and selective inhibition of HIV-1 replication in vitro by a novel series of TIBO derivatives. Nature **343:**470–474.

38. **Pierson, T. C., Y. Zhou, T. L. Kieffer, C. T. Ruff, C. Buck, and R. F. Siliciano.** 2002. Molecular characterization of preintegration latency in human immunodeficiency virus type 1 infection. J. Virol. **76:**8518–8531.

39. **Piliero, P. J.** 2004. Pharmacokinetic properties of nucleoside/nucleotide reverse transcriptase inhibitors. J. Acquir. Immune Defic. Syndr. **37**(Suppl. 1)**:**S2–S12.

40. **Sacha, J. B., and D. I. Watkins.** 2010. Synchronous infection of SIV and HIV in vitro for virology, immunology and vaccine-related studies. Nat. Protoc. **5:**239–246.

41. **Sato, M., T. Motomura, H. Aramaki, T. Matsuda, M. Yamashita, Y. Ito, H. Kawakami, Y. Matsuzaki, W. Watanabe, K. Yamataka, S. Ikeda, E. Kodama, M. Matsuoka, and H. Shinkai.** 2006. Novel HIV-1 integrase inhibitors derived from quinolone antibiotics. J. Med. Chem. **49:**1506–1508.

42. **Smith, P. F., R. DiCenzo, and G. D. Morse.** 2001. Clinical pharmacokinetics of non-nucleoside reverse transcriptase inhibitors. Clin. Pharmacokinet. **40:**893–905.

43. **Summa, V., A. Petrocchi, F. Bonelli, B. Crescenzi, M. Donghi, M. Ferrara, F. Fiore, C. Gardelli, O. Gonzalez Paz, D. J. Hazuda, P. Jones, O. Kinzel, R. Laufer, E. Monteagudo, E. Muraglia, E. Nizi, F. Orvieto, P. Pace, G. Pes-

catore, R. Scarpelli, K. Stillmock, M. V. Witmer, and M. Rowley.** 2008. Discovery of raltegravir, a potent, selective orally bioavailable HIV-integrase inhibitor for the treatment of HIV-AIDS infection. J. Med. Chem. **51:**5843–5855.

44. **Swiggard, W. J., C. Baytop, J. J. Yu, J. Dai, C. Li, R. Schretzenmair, T. Theodosopoulos, and U. O'Doherty.** 2005. Human immunodeficiency virus type 1 can establish latent infection in resting CD4+ T cells in the absence of activating stimuli. J. Virol. **79:**14179–14188.

45. **Tsibris, A. M., and M. S. Hirsch.** 2010. Antiretroviral therapy in the clinic. J. Virol. **84:**5458–5464.

46. **Wang, Y. J., P. M. McKenna, R. Hrin, P. Felock, M. Lu, K. G. Jones, C. A. Coburn, J. A. Grobler, D. J. Hazuda, M. D. Miller, and M. T. Lai.** 2010. Assessment of the susceptibility of mutant HIV-1 to antiviral agents. J. Virol. Methods **165:**230–237.

47. **Wenning, L., B.-Y. Nguyen, X. Sun, E. Hwang, Y. Chen, H. Teppler, C. Harvey, R. Rhodes, D. Ryan, N. Azrolan, and J. Stone.** 2008. Pharmacokinetic/pharmacodynamic (PK/PD) analyses for raltegravir (RAL) in phase II and III studies in treatment experienced HIV-infected patients, abstr. O_21. 9th Int. Workshop Pharmacol. HIV Ther., New Orleans, LA. Virology Education B.V., Utrecht, Netherlands.

48. **Young, S. D., S. F. Britcher, L. O. Tran, L. S. Payne, W. C. Lumma, T. A. Lyle, J. R. Huff, P. S. Anderson, D. B. Olsen, S. S. Carroll, D. J. Pettibone, J. A. O'Brien, R. G. Ball, S. K. Balani, J. H. Lin, I.-W. Chen, W. A. Schleif, V. V. Sardana, W. J. Long, V. W. Byrnes, and E. A. Emini.** 1995. L-743,726 (DMP-266): a novel, highly potent nonnucleoside inhibitor of the human immunodeficiency virus type 1 reverse transcriptase. Antimicrob. Agents Chemother. **39:**2602–2605.